DIGITALLY-TUNABLE MEMS FILTER USING MECHANICALLY-COUPLED RESONATOR ARRAY

Hengky Chandrahalim and Sunil A. Bhave
OxideMEMS Lab, Electrical and Computer Engineering, Cornell University, Ithaca, New York, USA

ABSTRACT

This paper reports on the design of a bandwidth-tunable RF MEMS filter using a series-coupled array of dielectrically-transduced square-extensional mode resonators. The proposed digital tuning scheme provides channel-agility and bandwidth granularity for analog spectral processors and RF spectrum analyzers. The resonators and filters are fabricated on the 3 µm thick device layer of a heavily doped SOI wafer with a 100 nm thick silicon nitride film sandwiched between the polysilicon electrodes and the silicon device layer. A 511 MHz overtone square-extensional mode resonator is demonstrated with a quality factor (Q) of 1,800 in air and motional impedance (R_X) of 1.1 kΩ. An array of four such resonators is coupled mechanically to form a channel-select filter with 1.4 MHz bandwidth at 509 MHz center frequency. By switching the DC-biasing scheme, the filter is split into narrower high and low sub-bands, each 700 kHz wide.

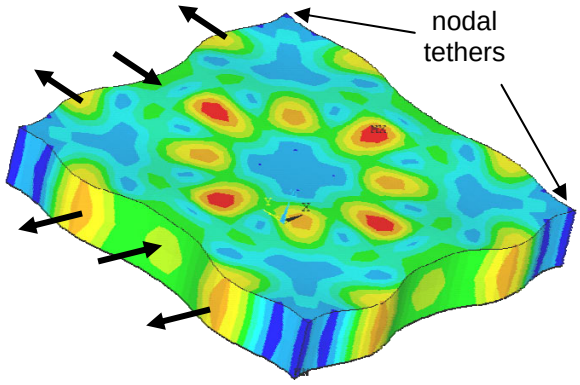

Figure 1: *ANSYS mode shape of a 3x3 overtone square-extensional resonator. The arrows indicate alternate square sections expanding and contracting.*

1. INTRODUCTION

Multi-band, multi-standard radio receivers such as next generation 7-band cellular phones and the joint task force radio system (JTRS) require a large array of channel-select filters connected in parallel. The input capacitance of the filter array will 'load' individual filters, deteriorating their stop-band rejection. Therefore, such frequency agile radios need multi-octave tunable band-select RF filters and bandwidth tunable channel-select IF filters with good shape factor and excellent stop-band rejection. An IF filter with dynamically tunable bandwidth will enable handling of multiple waveforms, eliminate out-of-channel interferers, and substantially decrease the number of filters in next-generation receivers.

Dielectrically-transduced thickness shear-mode resonators with analog voltage tunable center frequency and bandwidth are suitable candidates for channel-select IF filters [1]. The resonators require a back-side etch of the SOI substrate to pattern orthogonal frequency tuning electrodes and eliminate parasitic pad capacitance and resistive ground loops. However, such back-side processing is not compatible with the high-vacuum, ultra-clean epi-Silicon encapsulation technology [2] necessary for field deployment of these filters. Contour-mode MEMS resonators with Q > 5,000, low R_X , compatibility with epi-Silicon encapsulation and CAD-defined resonance frequencies from 10 MHz – 1GHz are excellent candidates for designing channel-select filter arrays [3]. But unlike thickness shear mode resonators, the frequency expressions for contour modes and flexural vibration modes do not directly couple. It is therefore difficult to perform orthogonal frequency tuning of contour-mode resonators. Since extensional mode resonators cannot be tuned at device-level (without excessive heating [4] or using liquid dielectric [5]), we implemented a tunable filter using a novel DC-biasing strategy in mechanically-coupled resonator array. This method does not require any frequency off-set between constituent resonators. As a result, lithography challenges are minimized, spatial distortion is greatly reduced and spurs in filter transmission are attenuated [6].

2. OVERTONE SQUARE-EXTENSIONAL MODE RESONATOR

MEMS resonators vibrating in a bulk-mode have superior linearity and high quality factors [7,8]. The bulk-extensional mode resonance of a square resonator depends on length L, with frequency $f = (n/2L)\sqrt{E/\rho}$ where E and ρ are effective elastic modulus for 2D expansion and density of the resonator respectively and n is the harmonic order (Figure 1). Higher frequency overtone modes are selectively excited by patterning electrodes in checkerboard configuration on top of the resonator using dielectric transduction.

Figure 2.a presents a 511 MHz resonator fabricated in a silicon nitride-on-silicon process [9]. The 100 nm silicon nitride film deposited on top of the resonator is sandwiched between the 3.1 µm thick silicon device layer and the 100nm thick conducting top electrodes. A 50V DC + small AC voltage is applied to the drive electrode and the silicon device layer is connected to RF ground. This time-varying voltage causes a squeezing force on the dielectric thin film. Due to the Poisson effect, the dielectric layer experiences a lateral strain. As the strain distributes through the resonator, the overtone square-extensional mode is excited.

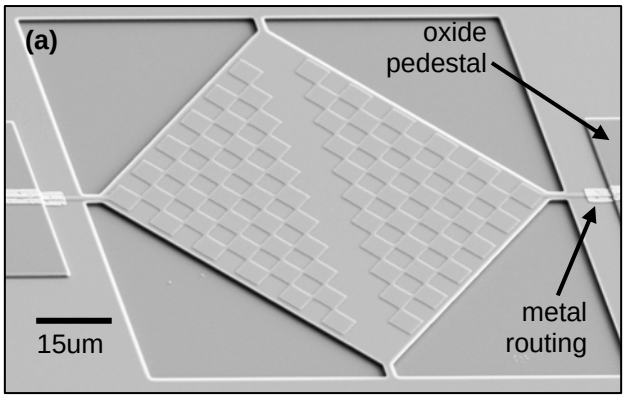

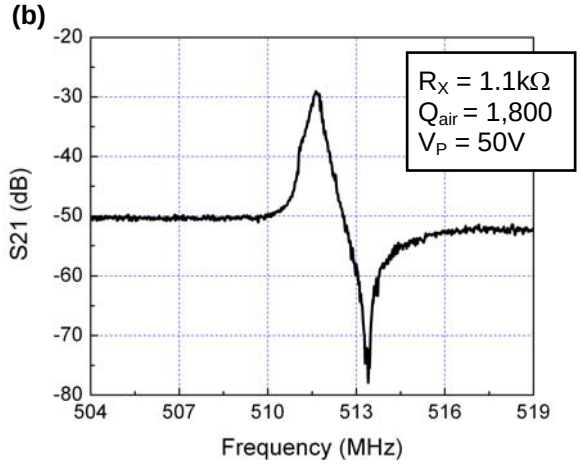

Figure 2: *(a) SEM of an overtone 2D square-extensional mode resonator with checkered electrodes for transduction. The resonator consists of a 100 nm SiN transducer sandwiched between poly electrodes and 3 µm thick silicon device layer. An oxide pedestal layer is added to the silicon nitride-on-silicon process to elevate the RF signal lines off the ground plane. Platinum metal traces and pads are introduced to improve RF signal integrity and reduce noise during probing. (b) Measured series resonance response of the resonator in air.*

Figure 3: *Four series mechanically-coupled checkered-electrode resonators. Each resonator has individually addressable RF+DC lines. The silicon device layer is an RF ground to prevent substrate losses. All RF paths are metalized, routed on an elevated oxide bridge to reduce capacitance and de-embedded to the edge of DRIE trench.*

The resonators were characterized in a RF probe station in a 2-port configuration using GSG probes. Parasitics up to the probe tips were first cancelled with SOLT measurements on a standard calibration substrate. De-embedding was then performed with Cascade WinCal software, using short, open, and through structures fabricated on-chip, but separate from the filters [10]. This de-embedding allows for the cancellation of the large pad capacitance without canceling out any parasitics inherent to the filters themselves, including suspension beam routing and transduction electrodes on the resonators. The measured transmission response has a motional impedance R_X of 1.1 kΩ and Q of 1800 in air (Figure 2.b).

3. DIGITALLY-TUNABLE FILTER

In multi-pole mechanically-coupled filters the resonators are coupled using quarter-wavelength suspensions (k_s) at low-velocity nodes. The quarter-wavelength springs minimize mass-loading of the resonators and low-velocity coupling enables narrow-bandwidth filter design with standard lithography tools. However, as we scale to radio frequencies the effective stiffness (k_r) and mass (m_r) of overtone mode resonators scale with the overtone order, minimizing filter distortion due to mass-loading and simplifying narrow-bandwidth filter design with coupled resonators at maximum-velocity locations.

Figure 3 shows a mechanically coupled four-pole filter consisting of overtone square-extensional resonators. The four vibration modes of the filter are [11] (Figure 4):

$$f_1 = \sqrt{k_r/m_r} \quad f_2 \approx \sqrt{(k_r + k_s)/m_r} \qquad (2)$$

$$f_3 \approx \sqrt{(k_r + 2k_s)/m_r} \quad f_4 \approx \sqrt{(k_r + 3k_s)/m_r}$$

Only the first and last resonators of multi-pole mechanically-coupled filters need to be electrostatically transduced. The intermediate resonators are mechanically coupled and DC biasing is not an absolute requirement. We retain individual control of the DC bias (V_P) for each resonator and exploit this property to implement digitally-tunable bandwidth channel-select filters. The programmable filter is configured as follows:

1. [DC1 = $+V_P$, DC2 = DC3 = OFF, DC4 = $+V_P$] – excites all 4 vibration modes and enables 4-port filter response.
2. [DC1 = DC3 = $+V_P$, DC2 = DC4 = $-V_P$] – excites the first two resonators out-of-phase. The system still has

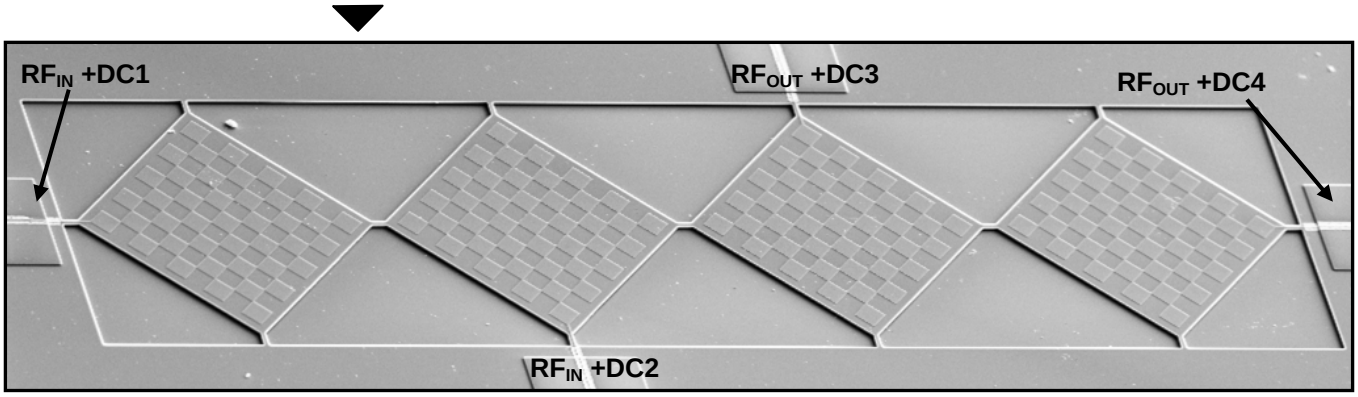

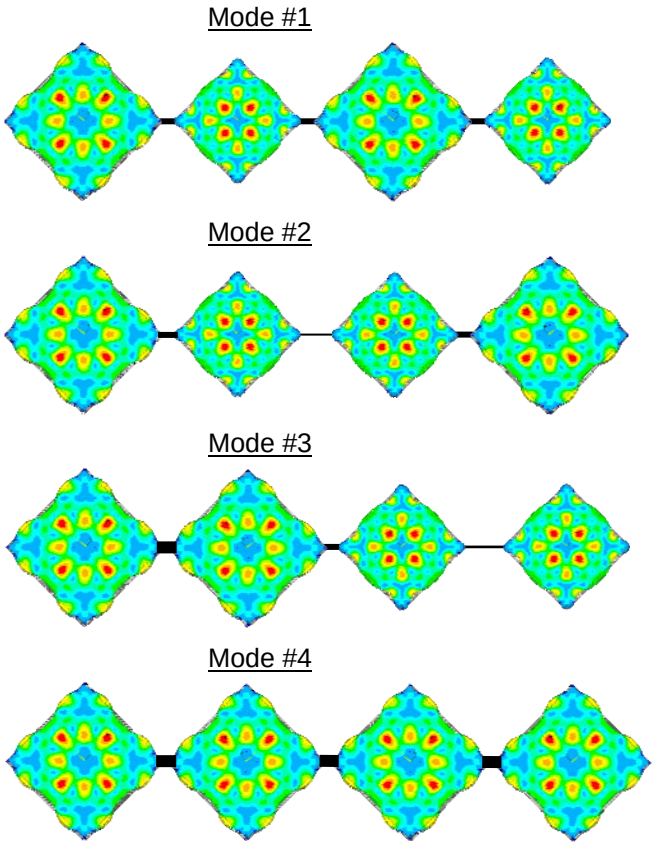

Figure 4: *Four vibration modes of a 4-pole filter consisting of overtone square-extensional mode resonators.*

four vibration modes, however the DC bias configuration attenuates the excitation of modes #3 and #4. In addition, the DC bias configuration of the last two resonators sums the out-of-phase motion of the resonators while nulling in-phase modes (and motional currents). The configuration results in a 2-pole lower sub-band filter.

3. [DC1 = DC2 = DC3 = DC4 = $+V_P$] – excites the first two resonators in-phase. This leads to exact inverse of the above configuration and results in a 2-pole higher sub-band filter.

4. EXPERIMENTAL RESULTS

To retain individual control of each transducer and reduce RF losses to the substrate, the silicon device layer is maintained at an RF ground and each RF I/O port has a superimposed independent DC supply. Calibration and de-embedding procedures to eliminate excessive probe-pad and substrate parasitics was performed prior to RF measurements [10]. The power-splitters and bias-Ts (DC=GND) for RF_{IN} and RF_{OUT} were included during de-embedding. The programmable filter is configured and characterized as follows:

1. [DC1 = 50V, DC2 = DC3 = 0V, DC4 = 50V] – enables a 4-pole filter with 1.4 MHz bandwidth at 508.7 MHz center frequency.
2. [DC1 = DC3 = 40V, DC2 = DC4 = -40V] – preferentially excites and senses the first two vibration modes which results in a 720 kHz bandwidth lower sub-band filter.
3. [DC1 = DC2 = DC3 = DC4 = 40V] – preferentially excites and senses the last two vibration modes which results in a 660 kHz bandwidth higher sub-band filter.

Figure 5 and Table 1 summarize the terminated filter response of each configuration. The DC bias for the sub-band filters was reduced to 40V to compensate for increased transducer area and ensure all filters have the same impedance for characterization.

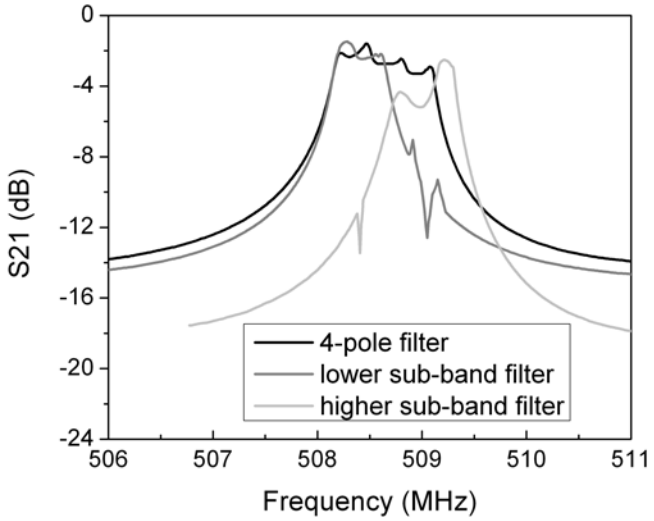

Figure 5: *Transmission response of three filters after termination using the PNA's pole-Z conversion function. The attenuated modes are clearly visible in the transmission response of the lower sub-band filter. The filter stop-band floor is high because electrical resistance in the ground plane leads to large capacitive feedthrough between drive and sense ports.*

Table 1: *Filter performance summary*

	4-pole filter	Lower sub-band filter	Higher sub-band filter
Insertion Loss	-2.4 dB	-2 dB	-3.1 dB
3dB Bandwidth	1.4 MHz	720 kHz	660 kHz
f_{CENTER}	508.7 MHz	508.3 MHz.	509.1 MHz
Ripple	< 2 dB	<1 dB	< 3 dB
stop band rejection	-14 dB	- 14 dB	-20 dB
DC Bias	50V on first and last resonators	40V and -40V on alternate resonators.	40V on all resonators
$R_{TERMINATION}$	4.1 kΩ	2.8 kΩ	2.9kΩ

5. CONCLUSION

In this work we demonstrated a digitally-tunable RF MEMS filter by controlling the DC bias voltages of individual resonators in a series coupled array. Using tri-state polarization voltage control ($-V_P$, GND, $+V_P$), the programmable filter provides bandwidth granularity for next generation frequency-agile radios. Although square-extensional and other contour-mode MEMS resonators are excellent candidates for designing channel-select filter arrays, they cannot be tuned significantly at the device level. By using the system-level digital-tuning scheme we have demonstrated a 4-pole filter consisting of four overtone square-extensional mode resonators at 509 MHz with 1.4 MHz bandwidth. By switching the DC polarization voltage of the individual resonators, the filter is split into narrower high and low sub-bands, each approximately 700 kHz wide. Due to limitations of the SOI fabrication process and resistive losses through the device layer, we were limited to four resonators and each RF I/O port had a superimposed independent DC supply. However, this can be easily resolved by switching to a surface-micromachining process [12]. Adding more resonators to the array will provide finer bandwidth granularity, however the maximum possible bandwidth is still limited by the coupling efficiency of the transducer.

6. ACKNOWLEDGMENTS

The authors wish to thank RF Micro Devices, Draper Laboratory, Rockwell Collins and DARPA/MTO's ASP program, whose generous support has made this research possible. We would also like to thank the Cornell NanoScale Science and Technology Facility (CNF) for resonator and filter fabrication.

7. REFERENCES

[1] L. F. Cheow, H. Chandrahalim, and S. A. Bhave, "MEMS filter with voltage-tunable center frequency and bandwidth," *Hilton Head 2006*, Hilton Head Island, SC, June 4-8, 2006, pp. 304-307.

[2] B. Kim, M. Hopcroft, C. M. Jha, R. Melamud, S. Chandorkar, M. Agarwal, K. L. Chen, W. T. Park, R. Candler, G. Yama, A. Partridge, M. Lutz, T. W. Kenny, "Using MEMS to build the device and the package," *Transducers'07*, Lyon, France, June 10-14, 2007, pp. 331-334.

[3] D. Weinstein, H. Chandrahalim, L. F. Cheow, and S. A. Bhave, "Dielectrically transduced single-ended to differential MEMS filter," *ISSCC 2006*, San Francisco, California, February 4-8, 2006, pp. 318-319.

[4] S. Pourkamali, and F. Ayazi, "High frequency low impedance capacitive silicon bar structures," *Hilton Head 2006*, Hilton Head Island, SC, June 4-8, 2006, pp. 284-287.

[5] H. Chandrahalim, S. A. Bhave, E. Quevy, and R. T. Howe, "Aqueous transduction of poly-SiGe disk resonators," *Transducers'07*, Lyon, France, June 10-14, 2007, pp. 313-316.

[6] S. -S. Li, Y. -W. Lin, Z. Ren, and C. T. -C. Nguyen, "A micromechanical parallel-class disk-array filter," *Frequency Control Symposium 2007*, Geneva, Switzerland, May 29-June 1, 2007, pp. 1356-1361.

[7] V. Kaajakari, T. Mattila, J. Kiihamäki, H. Kattelus, A.Oja, and H. Seppä, "Nonlinearities in single-crystal silicon micromechanical resonators," *Transducers'03*, Boston, MA, June 9-12, 2003, pp. 1574–1577.

[8] L. Khine, M. Palaniapan, and W.-K. Wong, "6MHz bulk-mode resonator with Q values exceeding one million," *Transducers'07*, Lyon, France, June 10-14, 2007, pp. 2445-2448.

[9] S.A. Bhave, and R.T. Howe, "Silicon nitride-on-silicon bar resonator using internal electrostatic transduction," *Transducers'05*, Seoul, Korea, June 5-9, 2005, pp. 2139-2142.

[10] M.-H. Cho, G.-W. Huang, C.-S. Chiu, K.-M. Chen, A.-S. Peng, and Y.-M. Teng, "A cascade open-short-thru (COST) de-embedding method for microwave on-wafer characterization and automatic measurement," *IEICE Transactions on Electronics* E88-C(5), pp. 845-850, 2005.

[11] P. Stephanou, "Piezoelectric Aluminum Nitride MEMS Resonators for RF Signal Processing," *Ph.D. Thesis*, University of California, Berkeley, December 2006, pp. 119-122.

[12] S.-S. Li, "Medium-scale integrated micromechanical filters for wireless communications," *Ph.D. Thesis*, University of Michigan, Ann Arbor, May 2007, pp. 180-182.